



Micronekton indicators evolution based on biophysically defined provinces

Authors: Sarah Albernhe^a, Thomas Gorgues^b, Olivier Titaud^a, Patrick Lehodey^c, Christophe Menkes^d, Anna Conchon^a

^a Collecte Localisation Satellites, 8-10 rue Hermès, Ramonville Saint Agne 31520, France

^b Univ Brest, CNRS, Ifremer, IRD, Laboratoire d'Océanographie Physique et Spatiale (LOPS), IUEM, F29280, Plouzané, France.

^c Mercator Ocean International, 2 Av. de l'Aérodrome de Montaudran, 31400, Toulouse, France

^d ENTROPIE, IRD, Univ. de La Réunion, CNRS, Ifremer, Univ. de la Nouvelle-Calédonie, BP A5, 98848 Nouméa, New Caledonia

Correspondence to: Sarah Albernhe (salbernhe@groupcls.com)

Abstract. Micronekton are mid-trophic marine organisms characterized by a size range of 2 to 20 cm, gathering a wide diversity of taxa (crustaceans, fish, molluscs, etc.). They are responsible for an important active carbon export to the deep ocean because of their diel vertical migrations and constitute the main prey for pelagic predators. A new method to define provinces that identify micronekton functioning patterns based on environmental variables is proposed in Albernhe et al. (2024, under review). Following this methodology, we define homogeneous provinces using environmental variables computed from Copernicus Marine Service products. These provinces represent a relevant way to define regions of interest, offering a regional scope of study for micronekton indicators and their evolution in time. In this study, we observe the evolution of the provinces in time from 1998 to 2023, to account for the seasonal to interannual variability. We focus on the variations in surface area and average latitude of each province. We observe a global shrinking of productive provinces and polar provinces, in favor of equatorial and tropical provinces expansion. Additionally, tracking the geographical changes of the provinces over time shows that most are shifting toward the poles.



41 1 Introduction

42 The intermediate level of the oceanic food web is constituted by a group of marine organisms called micronekton,
 43 understudied yet, but garnering increasing attention. This key component of marine ecosystems characterized by
 44 organisms in a size range from 2 to 20 cm contains a wide diversity of taxa such as crustaceans, fish, molluscs and
 45 gelatinous (Brodeur et al., 2004; Escobar-Flores et al., 2019). Micronekton mostly feed on zooplankton and are
 46 the main prey of marine large predators, some of which are of crucial economic importance (e.g. tunas, Bell et al.,
 47 2015; Terawasi et al., 2017; McCluney et al., 2019). In addition to their role of prey for commercially harvested
 48 top predators (Young et al., 2015), micronekton themselves become a valuable resource for fisheries, as the trophic
 49 level of exploited species is decreasing (St. John et al., 2016; Gatto et al., 2023). Another aspect of micronekton
 50 worthy of interest lies in its migratory behaviour, which impact global carbon export (Pinti et al. 2021; Buesseler
 51 et al., 2022) by actively transporting and sequestering carbon beneath the mixed layer (Bianchi et al., 2013; Boyd
 52 et al., 2019; Gorgues et al., 2019).

53 Therefore, estimating micronekton biomass is a major concern for fisheries management and climate regulation.
 54 Observations of micronekton primarily rely on trawl sampling, which is susceptible to biases due for example to
 55 species avoidance (Kaartvedt et al., 2012) or on ship-borne acoustic measurements, which does not provide yet a
 56 reliable representation of the micronekton biomass (McGehee et al., 1998; Kloser et al., 2002). Numerical models
 57 as the Spatial Ecosystem and Population Dynamics Model – Low and Mid Trophic Levels (SEAPODYM-LMTL:
 58 Lehodey et al., 2010; 2015; Conchon, 2016) are complementary tools for simulating micronekton biomass,
 59 offering the advantage of providing continuous global-scale time series.

60 One approach to quantify and characterize the mid-trophic level populations is the definition of homogeneous
 61 provinces. Longhurst was the pioneer and defined a static vision of biogeographical provinces based on
 62 chlorophyll fields (Longhurst 1995; 2007). Multiple combinations of environmental forcings have been used to
 63 create accurate definitions of provinces for each field: catch per unit of effort of commercial fisheries (Reygondeau
 64 et al., 2012), multi-expertise discussions (Sutton et al., 2017), distribution of species (Costello et al., 2017),
 65 phytoplankton species assemblages (Elizondo et al., 2021). Acoustic-based regionalization is also explored, using
 66 environmental drivers classification to model backscattering characteristics (Proud et al., 2017), or recently
 67 partitioning acoustic data according to the vertical structure of sound-scattering mid-trophic biomass (Ariza et al.,
 68 2022).

69 Complementing these approaches, Alberne et al. (2024, under review) proposed a new methodology for
 70 regionalizing the global ocean into biophysical provinces based on environmental variables. The ambition of this
 71 work was to identify micronekton homogeneous functioning patterns using a parsimonious set of biophysical
 72 variables that are known to have an impact on micronekton biomass (epipelagic layer temperature, stratification
 73 of the mesopelagic ocean, and net primary production (NPP)). Clustering these variables results in a global
 74 classification of six distinct biomes (tropical, subtropical, eastern boundary coastal upwelling systems, oceanic
 75 mesotrophic systems, sub-polar and polar biomes). The authors also defined a monthly time series of biomes for
 76 the 1998-2019 time period. From these large biomes, provinces are derived as biomes' sub-divisions at the scale
 77 of ocean basin and hemisphere. A characterization of these provinces with simulated micronekton from
 78 SEAPODYM-LMTL model outputs identifies biomes-specific relations between micronekton biomasses and the
 79 environmental variables used in the clustering. Additionally, biomes-specific vertical structures are indicated by
 80 ratios of modelled micronekton functional groups (i.e., groups of micronekton with specific migratory behaviour,
 81 and specific depth habitat). Boundaries between provinces have also been validated using acoustic data. With
 82 demonstrated accuracy in homogeneous micronekton characteristics, these provinces enable the gathering and
 83 extrapolation of the few available observation data of micronekton over large homogeneous areas. This could
 84 benefit the exploration of the micronekton spatio-temporal variability within global or regional datasets.

85 Provinces' features, such as surface area and positional changes, serve as valuable indicators offering insights into
 86 the evolution of ecosystem structure over time on both global and regional scales. Following Alberne et al. (2024,
 87 under review)'s methodology, we define in the present study an annual time series of biophysical provinces from
 88 1998 to 2023. We observe the evolution of two geographical indicators: the surface area and the average latitude
 89 of each province.

90

91

92



93 **2 Material and methods**

94 **2.1 Environmental variables and biophysical clustering**

95 We define a time series of biophysical provinces from 1998 to 2023 following Albernhe et al. (2024, under
 96 review)’s approach. The latter publication offers a methodology for global ocean regionalization based on
 97 environmental variables, with no gaps and no overlaps, displaying homogeneous biophysical characteristics.

98 We consider three environmental variables, that are known to have an impact on micronekton: the mean
 99 temperature in the epipelagic layer, the temperature gradient between the epi and the meso-pelagic layers, as an
 100 index of the stratification, and the integrated NPP. The pelagic layers mentioned are defined as in SEAPODYM-
 101 LMTL. These variables are computed from the biological and physical Copernicus Marine Service datasets of the
 102 product *Global Ocean low and mid trophic levels biomass content hindcast*,
 103 GLOBAL_MULTIYEAR_BGC_001_033 (1/12° horizontal resolution, product ref01, table 1). In the product, the
 104 weekly 3D temperature fields come from the GLORYS12V1 simulation. NPP and the associated euphotic depth
 105 are computed using the Vertically Generalized Production Model (VGPM) of Behrenfeld and Falkowski (1997)
 106 which is based on the Satellite Observations reprocessed Global Ocean Chlorophyll product. The spatial domain
 107 of our study is restricted to area where the depth of the water column supports the existence of all three pelagic
 108 layers as defined in SEAPODYM-LMTL (i.e. roughly 1000m deep, See Material and Method section of Albernhe
 109 et al. (2024, under review)). Consequently, shallow coastal areas are excluded from this analysis.

110 As described in Albernhe et al. (2024, under review), a Principal Component Analysis (PCA) (Hotelling, 1933) is
 111 performed on the three environmental variables mentioned above (i.e., epipelagic layer temperature, stratification
 112 and NPP). Then, a clustering is performed on the PCA two principal components, hereafter referred to as
 113 “biophysical clustering”. This biophysical clustering is performed using the unsupervised k-means machine
 114 learning algorithm (Lloyd, 1957; Pedregosa et al., 2011), which partitions the observations into $k=6$ homogeneous
 115 clusters (See Material and Method section of Albernhe et al. (2024, under review)). These clusters define
 116 homogeneous biomes on a global scale, hereafter referred to as “biophysical biomes”.

117 First, the training phase of k-means algorithm is applied to time-averaged 1/12-degree datasets from 1998 to 2023.
 118 This process defines static reference biophysical biomes, representing the average state of the ocean over the entire
 119 period. After the training phase, the clustering model parameters are estimated, and we can use this model to make
 120 predictions on other data. Then, the prediction phase of k-means algorithm is applied on monthly data over the
 121 same time period (1998-2023) (See Material and Method section of Albernhe et al. (2024, under review)). This
 122 results in a monthly time series of biophysical biomes that captures seasonal and interannual variability.

123 The biophysical biomes obtained from the clustering of environmental data characterize homogeneous
 124 environmental regimes on a global scale. In this study, we also delineate “provinces” as sub-divisions of biomes
 125 at the scale of ocean basins and hemispheres that have been shown to be characterized by stable biophysical drivers
 126 and potential taxonomic identity (Spalding et al., 2012; Sutton et al., 2017; Albernhe et al., 2024, under review).
 127 This subdivision enables the use of 27 provinces to define regional scopes for the study of micronekton.

128

129 **2.2 Trends identification**

130 The aim of this study is to observe the evolution of the provinces in time from 1998 to 2023. To study the
 131 interannual variability and identify potential trends over the 26 years, we consider the annual time series (i.e.,
 132 annually averaged monthly time series). We document the evolution of two geographical indicators: the surface
 133 area and the average latitude, for each province. The average latitude diagnostic has been designed to assess a
 134 potential poleward displacement of certain provinces (see Hastings et al., 2020; Pinsky et al. 2020 and references
 135 therein).

136 To evaluate the evolution of surface area over time, we analyze the slope (in km^2/year) of a linear regression model
 137 based on the annual surface area (in km^2) of each province from 1998 to 2023. The coefficient of determination
 138 (R^2) associated with every linear regression (i.e., computed for each province) is a statistical measure assessing
 139 the degree of alignment between the observed values and the linear regression model. From the linear regression,
 140 the percentage of variation of the provinces’ surface between 1998 and 2023 is computed (in %), based on the
 141 difference between the first and last point of the regression (respectively matching 1998 and 2023).

142 To track the poleward drift of provinces over time, we analyze the slope (in degrees poleward/year) of a linear
 143 regression model based on the average latitude of each province throughout the annual time series from 1998 to



2023. The coefficients of determination (R^2) associated with every linear regression are computed. The ‘degree poleward’ unit that we use for this diagnostic is associated with degree N for provinces in the northern hemisphere, and degree S for provinces in the southern hemisphere. Thus, provinces belonging to the equatorial Biome 1 (provinces 101, 102 and 103) are not considered in this diagnostic because of their equatorial position. Derived from the linear regressions, we estimate the poleward variation trend over the 26 years for each province (in degree poleward), based on the difference between the first and last point of the regression (respectively matching 1998 and 2023).

3 Results

3.1 Biophysical provinces definition

To define the homogeneous biophysical biomes, we perform a clustering on the two principal components generated by the PCA performed on the three environmental variables (i.e. epipelagic layer temperature, stratification and NPP). From the learning phase of the clustering algorithm, six static reference biophysical biomes (Figure 1) are defined on a global scale, representing the average state of the ocean over the entire period. The subdivision of these biomes according to ocean basin and hemisphere leads to the definition of 27 biophysical provinces (identified by different shades of the biomes’ colors in Figure 1).

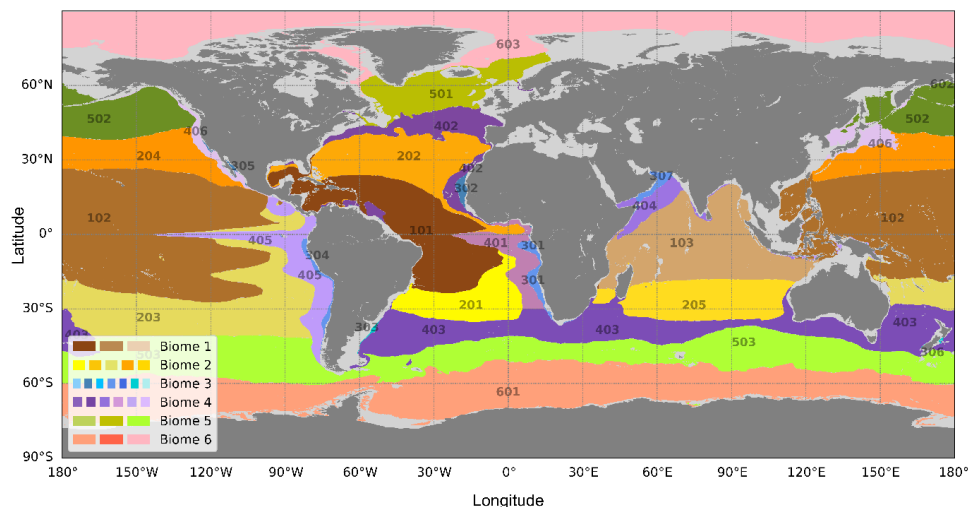


Figure 1: Map of reference biophysical biomes obtained by PCA principal component clustering from averaged epipelagic layer temperature, stratification, and NPP over the 1998-2023 time period. Geographical separation between different areas of the same biome defines 27 associated provinces. Provinces are identified by different shades of biomes’ colors, defined in the legend. One label is attributed to each province with the hundreds’ digits corresponding to the biome in which they belong. Grey areas delimitate the domain where the depth of the water column is not sufficient to ensure the existence of the three pelagic layers of SEAPODYM-LMTL (product ref 01, Table 1).

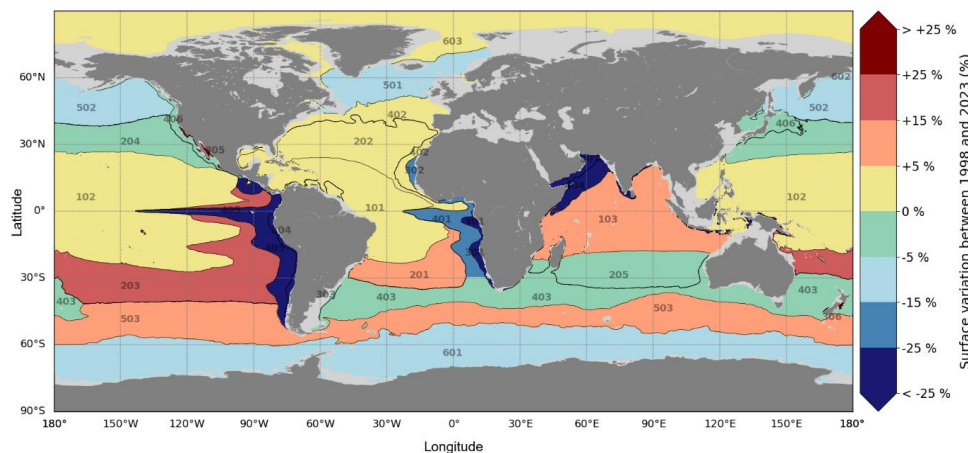
The six reference biophysical biomes are characterized as: tropical, subtropical, eastern boundary coastal upwelling systems, oceanic mesotrophic systems, sub-polar and polar (respectively numbered from 1 to 6). They are characterized by specific environmental regimes detailed in Alberne et al. (2024, under review).

The monthly time series of these provinces is available as an animation showing the provinces’ geographical evolution in time from 1998 to 2023 (<https://doi.org/10.5446/68853>). Together with the variations of ocean environmental conditions, the geographical extent of provinces evolves in time. Seasonal variability can be observed with the latitudinal shifts of the horizontal boundaries, as well as regional seasonal phenomena or isolated phenomena like ENSO events.



177 **3.2 Provinces' surface area evolution**

178 We aim to observe the geographical evolution of the provinces in time from 1998 to 2023. The slopes of the linear
179 regression models computed from the annual time series of surface area for each province are computed (See
180 supplementary material, Table S1, third column). These trends (in km²/year) are also expressed as the equivalent
181 percentage of evolution between 1998 and 2023, in % (Table S1, fourth column). The latter is displayed in Figure
182 2, as a map of the reference biophysical provinces showing their surface evolution in time from 1998 to 2023.



183 **Figure 2: Map of the provinces' surface area evolution in time from 1998 to 2023. Black lines delineate the definition of**
184 **the 27 reference biophysical provinces (cf. Figure 1). Colors represent the trend in surface variation for each province**
185 **(in % from 1998 to 2023): shades of red indicate increasing surface area, while shades of blue indicate decreasing surface**
186 **area.**
187

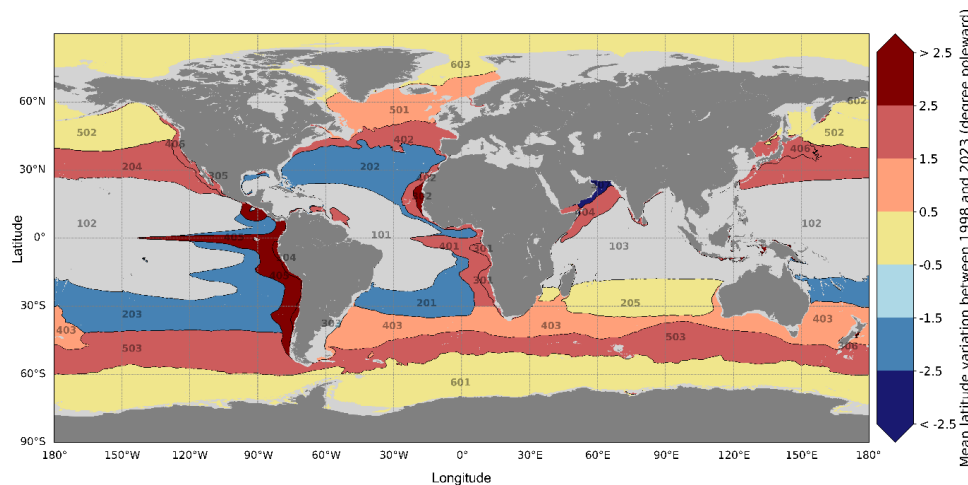
188 From 1998 to 2023, there has been a decline in the surface area of productive provinces (i.e., characterized by high
189 NPP) in eastern boundary coastal upwelling systems and oceanic mesotrophic systems (provinces belonging to
190 Biomes 3 and 4, i.e. labelled 300's and 400's), as indicated by the provinces colored with shades of blue in Figure
191 2. Most of the polar and subpolar provinces such as the North Atlantic and North Pacific subpolar areas
192 (respectively provinces 501 and 502) and the circumpolar province of the Southern Ocean (601) also display
193 decreasing trends in their extent. On the other hand, provinces with increasing surface trends are mostly tropical
194 or subtropical areas (Indian Ocean, South Atlantic tropical band, or South Pacific tropical band, respectively
195 provinces 103, 201 and 203).

196 On a global scale, productive provinces and polar provinces seem to shrink in favor of tropical provinces
197 expansion. However, some biomes exhibit significant discrepancies among the provinces they encompass. For
198 instance, the surface of the Southern Ocean province 503 (belonging to the subpolar Biome 5) shows an increasing
199 trend, in opposition with provinces 501 and 502 belonging to the same biome, showing decreasing trends in the
200 northern hemisphere.

201

202 **3.3 Provinces' average latitude evolution**

203 Together with the evolution of provinces' surface area, provinces' average latitude is a valuable metric to track the
204 geographical evolution of the provinces in time from 1998 to 2023. The slopes of the linear regression models
205 computed from the annual time series of average latitude for each province are computed (See supplementary
206 material, Table S2). The poleward displacement of each province between 1998 and 2023 is displayed in Figure 3
207 (in degree poleward).



208
209 **Figure 3: Map of the provinces' average latitude evolution in time from 1998 to 2023. Black lines display the definition**
210 **of the 27 reference biophysical provinces (cf. Figure 1). Colors represent the trend in average latitude variation for each**
211 **province (in degree poleward from 1998 to 2023): darker shades of red indicate poleward drifting, while darker shades**
212 **of blue indicate equatorward drifting. Provinces of the equatorial biome colored in grey (101, 102 and 103) are not**
213 **considered in this diagnostic because of their equatorial position.**

214 Most of the provinces experience poleward drifting (provinces colored with shades of red in Figure 3). The tropical
215 provinces displaying increasing surface trends (See provinces 201, 203, Figure 2) experience equatorward drifting,
216 as indicated by provinces colored with shades of blue in Figure 3. Provinces with average latitude evolution trends
217 between +0.5 and -0.5 degree poleward over the time period are considered as stable in time, in terms of latitude
218 (provinces colored in yellow in Figure 3).

219

220 3.4 Uncertainties

221 The robustness of the biophysical clustering obtained with the reference dataset, i.e., GLORYS12V1 for the
222 physical variables and VGPM for the biological variable (see section 2.1., and table 1, product ref01), is tested by
223 computing other biophysical clusterings derived from alternative environmental datasets. These alternative
224 datasets include physical data from ARMOR3D (Guinehut et al., 2012; Mulet et al., 2012) and biological data
225 from the biogeochemical model PISCES (Aumont et al., 2015),

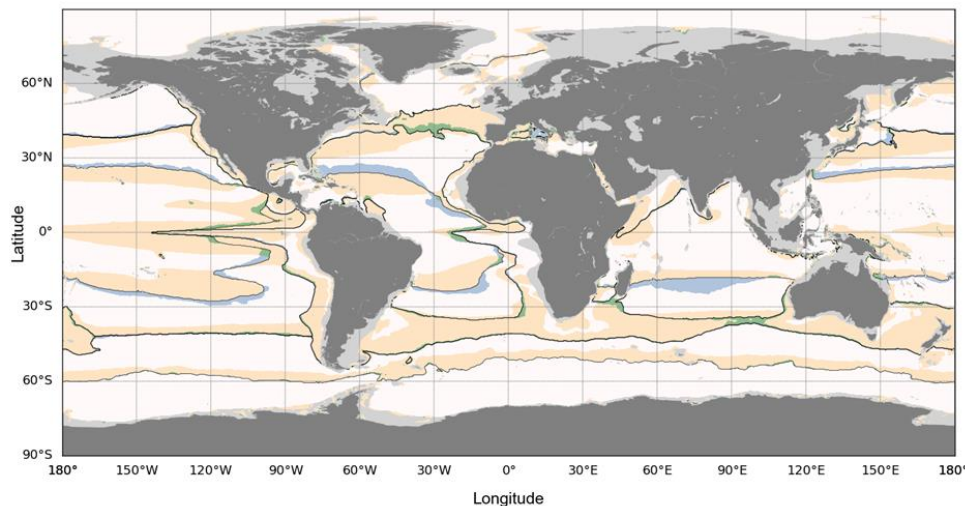
226 The *Multi Observation Global Ocean 3D Temperature Salinity Height Geostrophic Current and MLD* product of
227 Copernicus Marine Service (MULTIOBS_GLO_PHY_TSUV_3D_MYNRT_015_012, product ref03, table 1)
228 provides 3-D temperature from ARMOR3D dataset, derived from an optimal analysis of 3-D observations. This
229 product is used to compute the epipelagic layer temperature and the stratification, instead of GLORYS12V1 (used
230 in reference biophysical clustering, product ref01, table 1). A first alternative clustering, employing the same
231 methodology as the reference biophysical clustering (see II.1. Variables and biophysical clustering), is performed
232 using this product to compute the physical variables (the epipelagic layer temperature and the stratification), and
233 still using VGPM (product ref01, table 1) to compute the NPP.

234 Then, the *Biogeochemical hindcast for global ocean* product of Copernicus Marine Service
235 (GLOBAL_MULTIYEAR_BGC_001_029, product ref02, table 1), is used to compute the NPP variable for the
236 clustering instead of VGPM (product ref01, table 1). It provides 3D biogeochemical fields using PISCES
237 biogeochemical model outputs. A second alternative clustering, employing the same methodology as the reference
238 biophysical clustering, is performed using this product to compute the NPP, and still using GLORYS12V1
239 (product ref01, table 1) to compute the physical variables (as in the reference biophysical clustering).

240 The two alternative products mentioned above are available at ¼ degree from 1998 to 2022 at a monthly resolution.
241 Each of them is used to compute an alternative clustering (respectively using VGPM-ARMOR3D and PISCES-
242 GLORYS12V1). We compare our reference biophysical clustering (VGPM-GLORYS12V1, see Section 2.1),



243 downscaled from 1/12-degree to 1/4-degree resolution, with two alternative clusterings (Figure 4), all averaged
244 over the period 1998–2022.



245
246 **Figure 4: Clustering sensitivity analysis.** Map of reference biophysical biomes computed from GLORYS12V1 (product
247 ref01, table 1) and VGPM (product ref01, table 1), in black lines (cf. Figure 1). The white areas indicate where both
248 alternative clusterings assign the same cluster as the reference biophysical clustering. The blue areas indicate where the
249 clustering using ARMOR3D (product ref03, table 1) instead of GLORYS12V1 (product ref01, table 1) assign a different
250 cluster from the reference biophysical clustering. The yellow areas indicate where the clustering using PISCES (product
251 ref02, table 1) instead of VGPM (product ref01, table 1) assign a different cluster from the reference biophysical
252 clustering. The green areas indicate where both alternative clusterings assign a different cluster from the reference
253 biophysical clustering.

254 Figure 4 shows that the clustering is very stable when changing the physical variable source from GLORYS12V1
255 (product ref01, table 1) to ARMOR3D (product ref03, table 1), as blue areas highlight minor boundaries
256 differences. However, when changing biogeochemical variable source from VGPM (product ref01, table 1) to
257 PISCES (product ref02, table 1), the productive biome 4 is highly impacted. However, NPP estimations from
258 PISCES (product ref02, table 1) and VGPM (product ref01, table 1) differ significantly. We notice that the
259 clustering remains relatively stable with respect to the source of forcings, although variations can arise when
260 forcing fields differ widely. The time series and results presented in the study are thus valid using VGPM and
261 GLORYS12V1 (both product ref01, table 1), but caution should be taken in extrapolating those results to clusters
262 issued from other biogeochemical sources (e.g. models' outputs).

263

264 4 Discussion and conclusion

265 In this study, we defined an annual time series of biophysical provinces linked to micronekton from 1998 to 2023,
266 based on a methodology introduced in Albernhe et al. (2024, under review). In addition to the provinces' definition
267 methodology, this previous article demonstrates that each province features a specific characterization in terms of
268 micronekton biomass and vertical structure. Following the hypothesis that these characteristics are preserved over
269 time, which needs to be further investigated, the evolution of provinces' surface area can account for global
270 micronekton trends and estimations. For instance, the shrinking of provinces featuring the highest density of
271 micronekton biomass would lead to a global decrease of micronekton biomass.

272 In the present study, we observe a global shrinking of productive provinces and polar provinces, in favor of
273 equatorial and tropical provinces expansion (Figure 2). Productive provinces and subpolar provinces are
274 characterized by high densities of micronekton biomass (Albernhe et al., 2024, under review), whereas equatorial
275 and tropical ones display weaker densities. If provinces characteristics are preserved over time, these surfaces
276 variations imply a global decline of micronekton biomass. This potential trend for micronekton biomass evolution



277 on the historical period would be in range with studies on micronekton biomass climate projections (Bryndum-
278 Buchholz et al., 2018; Kwiatkowski et al, 2018; Lotze et al, 2019; Tittensor et al., 2021; Ariza et al., 2022).

279 The tracking of the geographical evolution of the provinces in time reveals that most of the provinces experience
280 poleward drifting (Figure 3). This poleward drifting is a valuable observation in range with the literature (Hastings
281 et al., 2020; Pinsky et al., 2020), suggesting a potential poleward migration of micronektonic populations induced
282 by temperature changes.

283

284

285

286

287

288

289

290

291

292

293

294

295

296

297

298

299

300

301

302

303

304

305

306

307

308

309

310

311

312 **Video supplement**



313 Sarah, Albernhe; Thomas, Gorgues; Olivier, Titaud; Patrick, Lehodey; Christophe, Menkes; Anna, Conchon:
 314 Biophysical provinces, monthly times series 1998-2023. Copernicus Publications, 2024.
 315 <https://doi.org/10.5446/68853>

316 Data availability

317 All data products used in this paper are listed in Table 1, along with their corresponding documentation and online
 318 availability.

319 **Table 1: Product Table**

Product ref. No.	Product ID & type	Data access	Documentation
01	GLOBAL_MULTIYEAR_BGC_001_033; Numerical Models	EU Copernicus Marine Service Product: <i>Global Ocean low and mid trophic levels biomass content hindcast</i> , Mercator Ocean International, https://doi.org/10.48670/moi-00020	Quality Information Document (QUID): Titaud et al., 2023 Product User Manual (PUM): Titaud et al., 2023
02	GLOBAL_MULTIYEAR_BGC_001_029; Numerical models	EU Copernicus Marine Service Product: <i>Biogeochemical hindcast for global ocean</i> , Mercator Ocean International, https://doi.org/10.48670/moi-00019	Quality Information Document (QUID): Perruche et al., 2019 Product User Manual (PUM) : Le Galloudec et al., 2022
03	MULTIOBS_GLO_PHY_TSUV_3D_MYNRT_015_012; In-situ observations, Satellite observations	EU Copernicus Marine Service Product: <i>Multi Observation Global Ocean 3D Temperature Salinity Height Geostrophic Current and MLD</i> , CLS, https://doi.org/10.48670/moi-00052	Quality Information Document (QUID): Greiner., 2023 Product User Manual (PUM) : Verbrugge et al., 2023

320

321 Author contributions

322 SA produced the clustering, the provinces' timeseries, and the associated diagnostic for their evolution in time.
 323 SA wrote and edited the report.

324 TG was involved in the investigation process as an advisor and reviewed the report.

325 OT was involved in the investigation process as an advisor and produced the lower and mid-trophic levels biomass
 326 density (*Global Ocean low and mid trophic levels biomass content hindcast*,
 327 GLOBAL_MULTIYEAR_BGC_001_033) 1998-2023 time-series.

328 The other authors are supervising the PhD of SA, and were involved in the investigation process to define the
 329 methodology used for the clustering (Albernhe et al., 2024, under review)



330 **Competing interests**

331 The contact author has declared that none of the authors has any competing interests.

332 **Disclaimer**

333 **Acknowledgements**

334 This work was funded by the NECCTON project, which has received funding from Horizon Europe RIA under
 335 grant agreement No 101081273.

336 **Financial support**

337 This work was partly funded by the GLO-RAN component of the Copernicus Marine Environment Monitoring
 338 Service (21003L04-COP-GLO RAN-4300) and the Horizon Europe RIA (Grant Number 101081273) & UK
 339 Research and Innovation NECCTON project.

340 **Review statement**

341 **References**

- 342 Ariza, A., Lengaigne, M., Menkes, C., Lebourges-Dhaussy, A., Receveur, A., Gorgues, T., ... & Bertrand, A.
 343 (2022). Global decline of pelagic fauna in a warmer ocean. *Nature Climate Change*, 12(10), 928-934.
- 344 Aumont, O., Éthé, C., Tagliabue, A., Bopp, L., & Gehlen, M. (2015). PISCES-v2: an ocean biogeochemical model
 345 for carbon and ecosystem studies. *Geoscientific Model Development Discussions*, 8(2), 1375-1509.
- 346 Bell, J. D., Allain, V., Allison, E. H., Andréfouët, S., Andrew, N. L., Batty, M. J., ... & Williams, P. (2015).
 347 Diversifying the use of tuna to improve food security and public health in Pacific Island countries and territories.
 348 *Marine Policy*, 51, 584-591.
- 349 Bianchi, D., Stock, C., Galbraith, E. D., & Sarmiento, J. L. (2013). Diel vertical migration: Ecological controls
 350 and impacts on the biological pump in a one-dimensional ocean model. *Global Biogeochemical Cycles*, 27(2),
 351 478-491.
- 352 Boyd, P. W., Claustre, H., Levy, M., Siegel, D. A., & Weber, T. (2019). Multi-faceted particle pumps drive carbon
 353 sequestration in the ocean. *Nature*, 568(7752), 327-335.
- 354 Brodeur, R. D., Seki, M. P., Pakhomov, E. A., and Suntssov, A. V. 2004. Micronekton - What are they and why are
 355 they important? *PICES Press*, 13: 7-11.
- 356 Bryndum-Buchholz, A., Tittensor, D. P., Blanchard, J. L., Cheung, W. W., Coll, M., Galbraith, E. D., ... & Lotze,
 357 H. K. (2019). Twenty-first-century climate change impacts on marine animal biomass and ecosystem structure
 358 across ocean basins. *Global change biology*, 25(2), 459-472.
- 359 Buesseler, K. O., Jin, D., Kourantidou, M., Levin, D. S., Ramakrishna, K., & Renaud, P. (2022). The ocean twilight
 360 zone's role in climate change. *Woods Hole Oceanographic Institution*.
- 361 Conchon, A. (2016). Modélisation du zooplancton et du micronekton marins (Doctoral dissertation, Université de
 362 La Rochelle).
- 363 Costello, M. J., Tsai, P., Wong, P. S., Cheung, A. K. L., Basher, Z., & Chaudhary, C. (2017). Marine biogeographic
 364 realms and species endemism. *Nature communications*, 8(1), 1057.
- 365 Elizondo, U. H., Righetti, D., Benedetti, F., & Vogt, M. (2021). Biome partitioning of the global ocean based on
 366 phytoplankton biogeography. *Progress in Oceanography*, 194, 102530.
- 367 Escobar-Flores, P. C., Ldroit, Y., and O'Driscoll, R. L. 2019. Acoustic assessment of the micronekton community
 368 on the Chatham Rise, New Zealand, using a semi-automated approach. *Frontiers in Marine Science*, 6: 507
- 369 Gatto, A., Sadik-Zada, E. R., Özbek, S., Kieu, H., & Huynh, N. T. N. (2023). Deep-sea fisheries as resilient
 370 bioeconomic systems for food and nutrition security and sustainable development. *Resources, Conservation and*
 371 *Recycling*, 197, 106907.



- 372 Gorgues, T., Aumont, O., & Memery, L. (2019). Simulated changes in the particulate carbon export efficiency due
 373 to diel vertical migration of zooplankton in the North Atlantic. *Geophysical Research Letters*, 46(10), 5387-5395
- 374 Guinehut, S., Dhomp, A. L., Larnicol, G., & Le Traon, P. Y. (2012). High resolution 3-D temperature and salinity
 375 fields derived from in situ and satellite observations. *Ocean Science*, 8(5), 845-857.
- 376 Hastings, R. A., Rutterford, L. A., Freer, J. J., Collins, R. A., Simpson, S. D., & Genner, M. J. (2020). Climate
 377 change drives poleward increases and equatorward declines in marine species. *Current Biology*, 30(8), 1572-1577.
- 378 Kaartvedt, S., Staby, A., & Aksnes, D. L. (2012). Efficient trawl avoidance by mesopelagic fishes causes large
 379 underestimation of their biomass. *Marine Ecology Progress Series*, 456, 1-6.
- 380 Kloser, R. J., Ryan, T., Sakov, P., Williams, A., & Koslow, J. A. (2002). Species identification in deep water using
 381 multiple acoustic frequencies. *Canadian Journal of Fisheries and Aquatic Sciences*, 59(6), 1065-1077.
- 382 Kwiatkowski, L., Aumont, O., & Bopp, L. (2019). Consistent trophic amplification of marine biomass declines
 383 under climate change. *Global change biology*, 25(1), 218-229.
- 384 Lehodey, P., Murtugudde, R., & Senina, I. (2010). Bridging the gap from ocean models to population dynamics
 385 of large marine predators: a model of mid-trophic functional groups. *Progress in Oceanography*, 54(1-2), 69-84.
- 386 Lehodey, P., Conchon, A., Senina, I., Domokos, R., Calmettes, B., Jouanno, J., ... & Kloser, R. (2015).
 387 Optimization of a micronekton model with acoustic data. *ICES Journal of Marine Science*, 72(5), 1399-1412.
- 388 Longhurst, A. (1995). Seasonal cycles of pelagic production and consumption. *Progress in oceanography*, 36(2),
 389 77-167.
- 390 Longhurst, A. (2007), *Ecological Geography of the Sea*, Academic Press, London.
- 391 Lotze, H. K., Tittensor, D. P., Bryndum-Buchholz, A., Eddy, T. D., Cheung, W. W., Galbraith, E. D., ... & Worm,
 392 B. (2019). Global ensemble projections reveal trophic amplification of ocean biomass declines with climate
 393 change. *Proceedings of the National Academy of Sciences*, 116(26), 12907-12912.
- 394 Lloyd, S. (1957). Least squares quantization in PCM. *IEEE transactions on information theory*, 28(2), 129-137,
 395 1982.
- 396 McCluney, J. K., Anderson, C. M., & Anderson, J. L. (2019). The fishery performance indicators for global tuna
 397 fisheries. *Nature communications*, 10(1), 1641.
- 398 McGehee, D. E., O'Driscoll, R. L., & Traykovski, L. M. (1998). Effects of orientation on acoustic scattering from
 399 Antarctic krill at 120 kHz. *Deep Sea Research Part II: Topical Studies in Oceanography*, 45(7), 1273-1294.
- 400 Mulet, S., Rio, M. H., Mignot, A., Guinehut, S. and Morrow, R.: A new estimate of the global 3D geostrophic
 401 ocean circulation based on satellite data and insitu measurements, *Deep. Res. Part II Top. Stud. Oceanogr.*, 77-80,
 402 70-81, doi:10.1016/j.dsr2.2012.04.012, 2012.
- 403 Pedregosa, F., Varoquaux, G., Gramfort, A., Michel, V., Thirion, B., Grisel, O., ... & Duchesnay, É. (2011). Scikit-
 404 learn: Machine learning in Python. *the Journal of machine Learning research*, 12, 2825-2830.
- 405 Pinsky, M. L., Selden, R. L., & Kitchel, Z. J. (2020). Climate-driven shifts in marine species ranges: Scaling from
 406 organisms to communities. *Annual review of marine science*, 12, 153-179.
- 407 Pinti, J., DeVries, T., Norin, T., Serra-Pompei, C., Proud, R., Siegel, D. A., ... & Visser, A. W. (2021). Metazoans,
 408 migrations, and the ocean's biological carbon pump. *BioRxiv*.
- 409 Proud, R., Cox, M. J., & Brierley, A. S. (2017). Biogeography of the global ocean's mesopelagic zone. *Current*
 410 *Biology*, 27(1), 113-119.
- 411 Reygondeau, G., Maury, O., Beaugrand, G., Fromentin, J. M., Fonteneau, A., & Cury, P. (2012). Biogeography
 412 of tuna and billfish communities. *Journal of Biogeography*, 39(1), 114-129.
- 413 Terawasi, P., & Reid, C. (2017). Economic and development indicators and statistics: Tuna fisheries of the western
 414 and central pacific ocean. In *Forum Fisheries Agency (FFA), Honiara*.



- 415 Spalding, M. D., Agostini, V. N., Rice, J., & Grant, S. M. (2012). Pelagic provinces of the world: A biogeographic
 416 classification of the world's surface pelagic waters. *Ocean & Coastal Management*, 60, 19-30.
- 417 St. John, M. A., Borja, A., Chust, G., Heath, M., Grigorov, I., Mariani, P., ... & Santos, R. S. (2016). A dark hole
 418 in our understanding of marine ecosystems and their services: perspectives from the mesopelagic community.
 419 *Frontiers in Marine Science*, 3, 31.
- 420 Sutton, T. T., Clark, M. R., Dunn, D. C., Halpin, P. N., Rogers, A. D., Guinotte, J., ... & Heino, M. (2017). A
 421 global biogeographic classification of the mesopelagic zone. *Deep Sea Research Part I: Oceanographic Research*
 422 *Papers*, 126, 85-102.
- 423 Tittensor, D. P., Novaglio, C., Harrison, C. S., Heneghan, R. F., Barrier, N., Bianchi, D., ... & Blanchard, J. L.
 424 (2021). Next-generation ensemble projections reveal higher climate risks for marine ecosystems. *Nature Climate*
 425 *Change*, 11(11), 973-981.
- 426 Young, J. W., Hunt, B. P. V., Cook, T. R., Llopiz, J. K., Hazen, E. L., Pethybridge, H. R., Ceccarelli, D., et al.
 427 2015. The trophodynamics of marine top predators: Current knowledge, recent advances and challenges. *Deep Sea*
 428 *Research Part II: Topical Studies in Oceanography*, 113: 170–187.